

Research paper

# Elimination of sulfates from wastewaters by natural aluminosilicate modified with uric acid

J. De Los Santos <sup>a</sup>, J.M. Cornejo-Bravo <sup>a</sup>, E. Castillo <sup>a</sup>, N. Bogdanchikova <sup>b,\*</sup>, S.M. Farías <sup>b</sup>, J.D. Mota-Morales <sup>c</sup>, E.S. Reynoso <sup>d</sup>, A. Pestryakov <sup>e</sup>, J.G. Rodríguez Ventura <sup>a</sup>

<sup>a</sup> *Facultad de Ciencias Químicas e Ingeniería, Universidad Autónoma de Baja California, Tijuana, B.C., Mexico*

<sup>b</sup> *Centro de Nanociencias y Nanotecnología, UNAM, Ensenada, B.C., Mexico*

<sup>c</sup> *Conacyt Research Fellow at Centro de Nanociencias y Nanotecnología-UNAM, Ensenada, B.C., Mexico*

<sup>d</sup> *Instituto Tecnológico de Tijuana, Centro de Graduados e Investigación en Química e Ing. Nanotecnología, Tijuana, B.C., Mexico*

<sup>e</sup> *Tomsk Polytechnic University, Tomsk 634050, Russia*

Received 6 October 2015; received in revised form 11 November 2015; accepted 17 November 2015

Available online 14 December 2015

## Abstract

Natural aluminosilicate activated by a heat/acid treatment, followed by modification with uric acid was used to remove sulfates for treatment of wastewater effluent. Natural aluminosilicates were studied in every stage of the modification (namely activation, modification with uric acid, and after sulfates absorption) by scanning electron microscopy (SEM), spectroscopy X-ray diffraction (XRD), energy dispersive spectroscopy (EDS), surface area (BET), X-ray photoelectron spectroscopy (XPS), thermogravimetric analysis (TGA), and Z potential. More than 60% of the initial concentration of sulfates (500 mg/l) was removed with the natural aluminosilicate modified with uric acid. Absorption isotherms rendered a mechanism with contributions from both Langmuir and Freundlich mechanisms. This study opens the path for the use of natural and abundant local material to remove sulfates using a modifier already present in wastewater effluents as contaminant.

© 2015 Tomsk Polytechnic University. Production and hosting by Elsevier B.V. This is an open access article under the CC BY-NC-ND license (<http://creativecommons.org/licenses/by-nc-nd/4.0/>). Peer review under responsibility of Tomsk Polytechnic University.

**Keywords:** Natural aluminosilicate; Uric acid; Sulfates; Isotherms; Adsorption

## 1. Introduction

The main limitation for reusing reclaimed water is its low quality in terms of nitrogen-based nutrients (NH<sub>3</sub>, NO<sub>2</sub><sup>-</sup>, NO<sub>3</sub><sup>-</sup>), phosphates (PO<sub>4</sub><sup>-3</sup>) and sulfates (SO<sub>4</sub><sup>-2</sup>), which precludes its use in recharging local groundwater aquifer [1]. According to World Health Organization [2], a global network of water monitoring stations, typical sulfate levels in fresh water are in the vicinity of 20 mg/l and range from 0 to 630 mg/l in rivers (the highest values are found in Belgium and Mexico), from 2 to 250 mg/l in lakes (the highest value is found in Mexico) and from 0 to 230 mg/l in groundwater (the highest values are found in Chile and Morocco). In 1970, the US Public Health Service measured sulfate levels in the drinking-water sources of nine

geographic areas. Sulfate was found to be present in 645 of 658 groundwater supplies and in all of the 106 surface water supplies sampled. Sulfate levels ranged from <1 to 770 mg/l, with a median of 4.6 mg/l. Only 3% of the water supplies sampled had sulfate levels in excess of 250 mg/l.

With an average annual precipitation of 273 mm and a rapid population growth, the region of Tijuana–San Diego, in the Mexico–USA border, is currently experiencing a scarcity of water resources [3]. In Tijuana, local wastewater treatment plant system (WWTPS) generates 79.65 Mm<sup>3</sup>/year (2590 lps) of reclaimed water, from which 0.11 Mm<sup>3</sup>/year (85.03 lps) is used for irrigation and the rest is discharged to the Pacific Ocean and thus not utilized [4]. Therefore strategies aimed to increase the quality of reclaimed water are a must. Adsorption and ion exchange stand as the most effective technologies and economic alternatives for removing contaminants from water. Previous studies for pollutants removal of reclaimed water with aluminosilicates, zeolites [5] and activated calcite [6], showed high efficiency for nitrogen and phosphates removal; however that is not the case for sulfates.

\* Corresponding author. Centro de Nanociencias y Nanotecnología, Universidad Nacional Autónoma de México, Ensenada 22860, Mexico. Tel.: +52 (646) 175 0650; fax: (646) 174 4603.

E-mail address: [nina@cnyun.unam.mx](mailto:nina@cnyun.unam.mx) (N. Bogdanchikova).

<http://dx.doi.org/10.1016/j.reffit.2015.11.003>

2405-6537/© 2015 Tomsk Polytechnic University. Production and hosting by Elsevier B.V. This is an open access article under the CC BY-NC-ND license (<http://creativecommons.org/licenses/by-nc-nd/4.0/>). Peer review under responsibility of Tomsk Polytechnic University.

Technologies involving reverse osmosis [7], electrochemistry [8], biotechnology, adsorption and ion exchange [9,10] have been applied to control pollution caused by sulfates. Among the preferred absorbers, natural aluminosilicates are the most widely used due to its low cost, ample distribution and preference for specific contaminants [11–13]. During the last twenty years numerous researchers have been working on the creation of adsorption materials based on modified aluminosilicates. Common modifications include the use of acids, bases, cationic surfactants and polioxocations [14,15]. Intercalation routes, organic molecules located in the interlayer space, post-synthesis grafting of organosilane onto aluminosilicate surfaces [16,17] and one step preparation of aluminosilicates by sol–gel process [18,19] have been also used. Natural aluminosilicate (bentonite) is a widespread type of clay that can be easily modified with quaternary ammonium salts for applications in many fields, including sulfate remove from water [20]. Recent reports showed the capacity of bentonite to adsorb uric acid and creatinine in rats thus inhibiting their adsorption in the intestine [21].

In some regions (e.g. Tijuana–Otay, Mexico–USA border) soil possess high content of natural aluminosilicate (bentonite) and other aluminosilicates [22]. The aim of this study was to use a natural aluminosilicate-type material to remove uric acid and sulfate solutions that emulate treated wastewater effluent through two steps: (1) Uric acid absorption into natural aluminosilicate as modifier of the surface properties (e.g. charge), (2) adsorption of  $\text{SO}_4^{2-}$  in the modified aluminosilicate with uric acid. The method here described introduces preliminary results regarding a low cost alternative for the reuse of wastewater, which takes advantage that both the modifier and the sulfates are already present in domestic and industrial wastewater effluents.

## 2. Materials and methods

### 2.1. Materials

#### 2.1.1. Natural aluminosilicate

The natural aluminosilicate was collected by gravimetric sedimentation and passed through No. 635 mesh ASTM Standard Testing Sieve vibrator E-11, model 150 [23]. Then, the sample was washed with distilled water and dried at 100 °C. The sample was labeled NA, which stands for natural aluminosilicate.

#### 2.2. Activation of natural aluminosilicate (NA)

Twenty-five grams of natural aluminosilicate (NA) was dispersed into 250 ml of hydrochloric acid 2N, at 90 °C for 2 hours, afterwards it was washed with 3 l water and dried at 250 °C for 4 h [24]. The sample was labeled AA (activated aluminosilicate). The cation exchange capacity of NA was determined by the copper ethylene diamine complex ( $\text{Cu}(\text{EDA})_2^{+2}$ ) method [25].

#### 2.3. Adsorption kinetic of uric acid into activated aluminosilicate (AA)

A sample of 600 mg of AA was added to 50 ml of uric acid solution ( $113 \text{ mg l}^{-1}$ ) under magnetic stirring in a 250 ml Pyrex glass flask at 25 °C; hydrochloric acid solution (2N) was used to

adjust the pH to 2.0 (Orion type PHS-25C). Uric acid absorption on the filtrates was measured after 5, 15, 30, 60, 90 and 120 min on different samples. The resultant sediment was filtered and centrifuged. The remained uric acid in solution was determined by an enzymatic–colorimetric method (diagnostic ELITECH) at  $\lambda = 550 \text{ nm}$  with a spectrophotometer DR.5000 HACH, thus the uric acid uptake was calculated by the difference between the initial and final concentrations of uric acid in solution after absorption on the aluminosilicate.

#### 2.4. Effect of pH on the uric acid absorption on AA

Two hundred fifty milliliters of a uric acid solution with an initial concentration of  $400 \text{ mg l}^{-1}$  was added to different masses of AA (from 0.1 to 1.0 g) in stopped Pyrex glass flasks under magnetic stirring at 25 °C. Hydrochloric acid solution (2N) was used to adjust the pH to 2 followed by agitation by 30 min at 89 rpm. The absorption of uric acid at different pH was calculated by measuring the concentration of uric acid remained in the solution after the filtration of the aluminosilicate (enzymatic–colorimetric method using diagnostic ELITECH at  $\lambda = 550 \text{ nm}$  with a spectrophotometer DR.5000 HACH). The same approach was used with pH 7 and 10, adjusting the pH with a sodium hydroxide solution 2N.

#### 2.5. Preparation of modified aluminosilicate with uric acid (AA-U)

Five grams of AA was dispersed into 250 ml of uric acid solution ( $600 \text{ mg l}^{-1}$ ) and heated to 80 °C for 1 h. Then the aluminosilicate, now modified with uric acid (AA-U), was washed with 3 l of deionized water followed by addition of 200 ml of hydrochloric acid (7N). The modified aluminosilicate was finally centrifuged and dried at 60 °C for 24 hours [21,24]. The sample was labeled AA-U.

#### 2.6. Adsorption kinetic of sulfates on AA-U

A sample of 1 g of AA-U was added to 200 ml of sodium sulfate solution ( $500 \text{ mg l}^{-1}$ ) under magnetic stirring in a 250 ml Pyrex glass flask at 25 °C; sodium hydroxide (2N) was used to adjust the pH to 7.0 (Orion type PHS-25C). Sulfates absorption on the filtrates was measured after 20, 40, 60, 80, 100, and 120 min on different samples. The resultant sediment was filtered and centrifuged. The amount of sulfates removed by the AA-U was calculated measuring the concentration of sulfate ion remained in the supernatant after centrifugation and concentration of sulfate ion initial.

#### 2.7. Absorption of sulfates on AA-U

Five grams of AA-U was used as absorbent material in 200 ml of sodium sulfate with concentration ranging from 200 to  $500 \text{ mg ml}^{-1}$  at pH 7. The samples were stirred in a rotatory equipment Jar Tester Unit programmable Phipps & Bird series PB-900 at 89 rpm and  $25 \text{ °C} \pm 2 \text{ °C}$ , for 120 minutes. The samples were then filtered and centrifuged (VWR clinical 50 centrifuge). The amount of sulfates removed by the AA-U was calculated measuring the concentration of sulfate ion remained in the supernatant after centrifugation. The method employed

was based on a colorimetric reaction of sulfates with Barium at 450 nm (SulfaVer 8051 Hach).

### 2.8. Characterization of NA, AA-U and the product after sulfate adsorption (AA-US)

X-ray diffraction patterns were conducted using the powder diffraction procedure [26]. Sample was ground in a small agate mortar. Powder X-ray diffraction patterns were recorded on a Bruker AXS diffractometer (CuK $\alpha$ , step size 0.01 $^\circ$ , counting time per step of 2 s). The surface composition of samples was evaluated by means of X-ray photoelectron spectroscopy (XPS) brand high resolution SPECS employing an Mg anode with characteristic X-ray energy of 1253 eV. The morphologies of natural aluminosilicate (NA), modified NA (AA-U) and AA-U with adsorbed sulfates (AA-US) were studied by scanning electron microscopy (JEOL JSM-5300), and the elements were quantified by energy dispersive spectroscopy (JEOL JIB-4500). Surface areas of NA and AA were measured by adsorption of nitrogen according to the BET-method on a Micrometrics Gemini 2360 apparatus. Thermogravimetric analysis (TGA) of samples NA, AA, AA-U and AA-US was performed by TGA Q500 V20.13 Build 39 instrument at a heating rate of 10  $^\circ\text{C min}^{-1}$  in a temperature range from room temperature up to 900  $^\circ\text{C}$ , in an inert atmosphere of nitrogen. Sample mass was around 4 mg. Zeta potential measurements of materials AA, AA-U, AA-US were done with a Zetasizer Nano-ZS, ZEN-3500 model, Malvern Instruments (England). The device uses laser green light of 532 nm/50 mW.

## 3. Results and discussion

The elemental analyses by EDS for different samples are summarized in Table 1. It can be observed that in the natural aluminosilicate (NA) the aluminum and silicon content, i.e. the ratio Al to Si is 3.3. Other significant elements presented are Fe (2.9%) and to a lesser extent K, Ca and Ti. When NA was modified with uric acid (AA-U) a decrease in Al, Si, K, Na, Ca and Fe is observed, this is due to the activation made on NA previously to uric acid modification. During the activation treatment, which involves heat and acid pH, impurities and cations are washed out and Al can also be partially eliminated from the octahedral structure of aluminosilicate [24]. It is worthy to note

Table 1

Composition by energy dispersive spectroscopy (EDS) for natural aluminosilicate (NA), modified NA with uric acid (AA-U) and sulfates adsorbed on modified aluminosilicate with uric acid (AA-US).

Atomic %	NA	AA-U	AA-US
O	64.33	66.44	65.22
Al	7.08	5.16	4.85
Si	23.82	23.38	27.3
K	0.87	0.56	0.66
Ca	0.7	0.18	0.23
Ti	0.28	0.31	0.36
Fe	2.91	1.52	1.38
S	–	–	1.12
Na	0.02	–	–

that activated aluminosilicate modified with uric acid (AA-U) shows up to 1.12% of sulfur after sulfate adsorption.

Regarding the nitrogen content, XPS analysis was performed because elemental analysis by EDS was unable to detect N in the samples. Monitoring the presence of N constitutes an exact approach to detecting indirectly the presence of uric acid. In the XPS spectra on Fig. 1, nitrogen is noticeable at the binding energy of 406.5 eV that corresponds to the N 1s peak characteristic of amines.

Fig. 2 shows the X-ray diffraction patterns of the aluminosilicate at different stages of the processing, namely raw material NA, activated AA, modified with uric acid AA-U, and with sulfates absorbed AA-US. A high content of quartz located at angles  $2\theta = 26.61$  and  $50.07$  [27–29]. Note that sulfate adsorption does not change the crystal structure of activated aluminosilicate (AA).

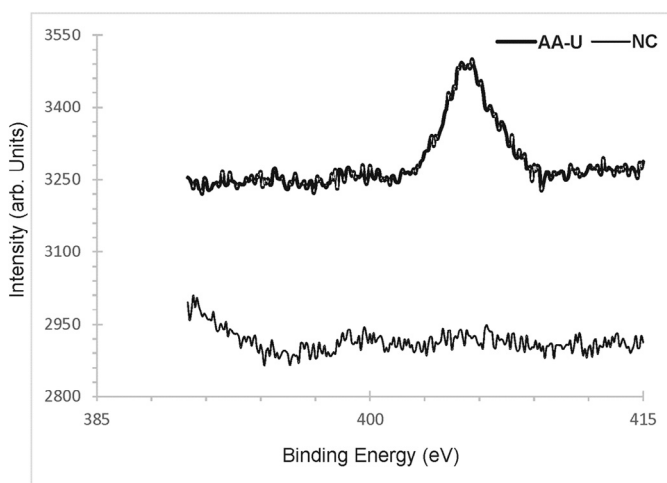


Fig. 1. Comparison of X-ray photoelectron spectroscopy results in the N 1s region for natural aluminosilicate (NA) and modified aluminosilicate with uric acid (AA-U).

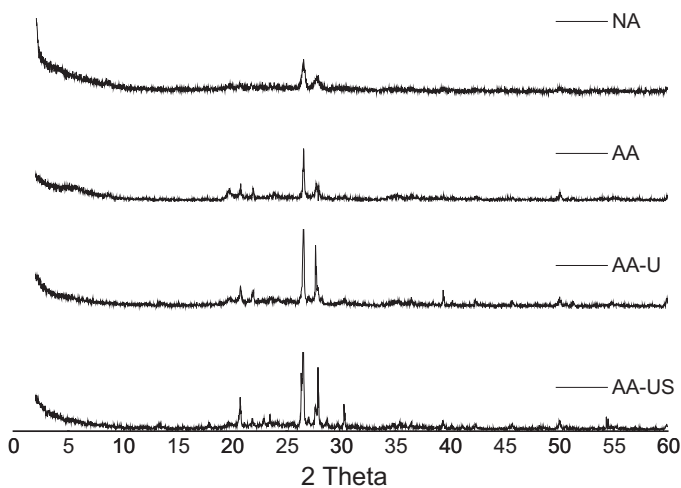


Fig. 2. X-ray diffraction for raw natural aluminosilicate (NA), activated aluminosilicate (AA), modified aluminosilicate with uric acid (AA-U) and sulfates adsorbed on modified aluminosilicate with uric acid (AA-US).



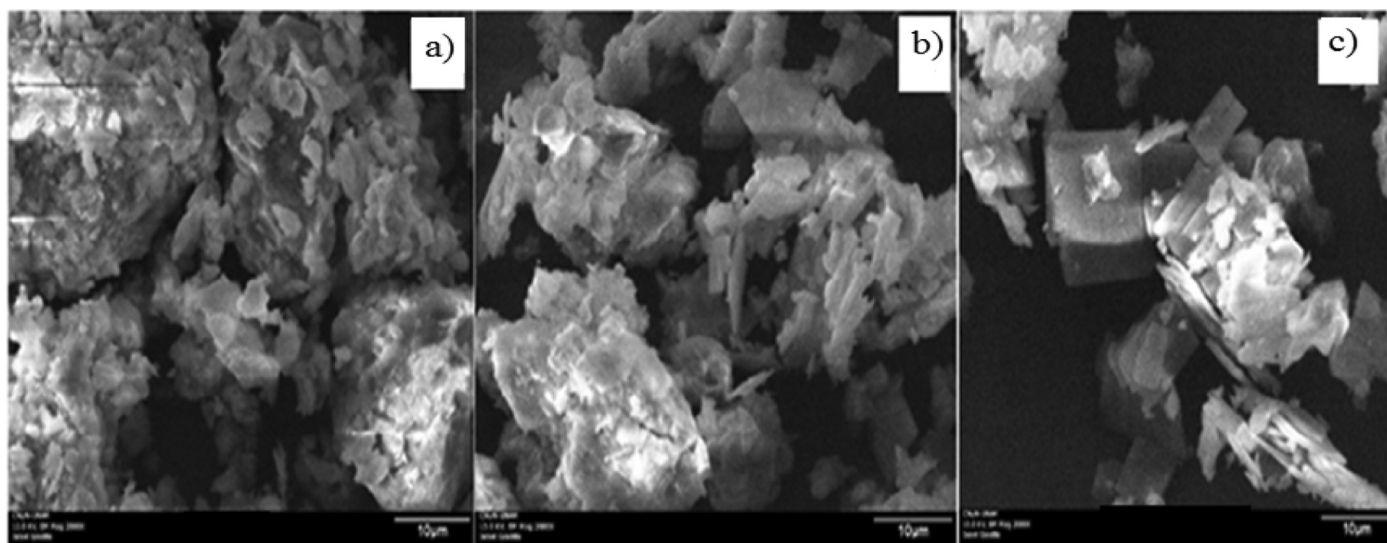


Fig. 3. Scanning electron microscopy images of (a) activated aluminosilicate (AA), (b) aluminosilicate modified with uric acid (AA-U), (c) sulfates adsorbed on modified aluminosilicate with uric acid (AA-US).

Micrographs using SEM show that NA samples presented different grain sizes compared to that in the natural aluminosilicate after activation (Fig. 3). The former comprises aggregates of irregularly shaped particle grains with diameter of ca. 4  $\mu\text{m}$ , which are formed by several flake-like particles randomly stacked. On the other hand, in Fig. 3b and c, AA-U and AA-US respectively, it can be observed that particle size increases to ca. 10  $\mu\text{m}$  showing pill-like plaques with more ordering and exposed edges.

Surface area (BET) of bare NA was 66.1  $\text{m}^2 \text{g}^{-1}$ . After the activation treatment with hydrochloric acid and heat, the surface area greatly increases to 141.05  $\text{m}^2 \text{g}^{-1}$  as well as pore volume. This is in accordance with the fact that washing out impurities (e.g. carbonates and amorphous material) and partial elimination of Al from interstitial octahedral structure increase microporosity (Table 2). However these results are far less than the surface area reported from other aluminosilicates (bentonites), which pose surface area of about 800  $\text{m}^2 \text{g}^{-1}$  [30], emphasizing the source of this aluminosilicate naturally occurring. Surface area of both AA-U and AA-US was not possible to be evaluated by this method because of the volatile nature of the organic modifier that decomposes during the treatment prior measurement.

Fig. 4 shows thermogravimetric analysis (TGA) traces of the different materials.

Comparing the TGA traces of NA and AC, it is evident that after activation, the resulting materials (AA) presented less

moisture and impurities (accounting for 3% wt.). For instance, the first step occurring before 150  $^{\circ}\text{C}$  is ascribed to water absorbed in the aluminosilicate and volatile compounds evaporation, while the second step around 450  $^{\circ}\text{C}$  can be due to dehydroxilation. In the case of NA modified with uric acid (AA-U) and the samples resulting from adsorption of sulfates (AA-US), three main steps are visible. As well as NA and AA, the first step is related with loss of water. However, around 300  $^{\circ}\text{C}$  uric acid presented in AA-U start decomposing, and finally at 400  $^{\circ}\text{C}$  the last weight loss step occurs in the same way that in the AA. In the sample containing uric acid and sulfates (AA-US), the second step is more prominent than in the previous samples evidencing a high load of material decomposing at this temperature. Because this lost of weight occurs in the same region that uric acid in AA-U, one can conclude that sulfates and uric acid begin decomposing during the range of temperature. By comparing the remained weight of each sample it is clear that AA-US lost around 15% more weight than AA-U, which in turns lost ca. 7.5% more weight than AA.

Z potential of materials in solution was evaluated to get insight about the surface charge as a result of modifications introduced by activation, uric acid integration and finally after sulfate adsorption. In Table 3 values for Z potential are reported. The activated natural aluminosilicate has a value of Z potential of  $-36.9 \text{ mV}$ , which is characteristic of c aluminosilicate having normally isomorphous substitutions in their structure, as was inferred to occur by the acid/heating treatment. Upon incorporation of uric acid, Z potential of the aluminosilicate drops to  $-13 \text{ mV}$ , indicative of neutralization of negative sites by uric acid. Uric acid has actually two pKa at 4.5 and 10.3, so it is plausible that strong interactions between negative sites in the surface of the NA and protons of partially charged uric acid can be readily established [31]. Finally, adsorbed sulfates decrease the Z potential to  $-18 \text{ mV}$ , presumably due to its accommodation via electrostatic interactions over uric acid already interacting with aluminosilicate surface.

Table 2  
Surface area (BET) of natural aluminosilicate (NA) and activated aluminosilicate (AA).

Sample	Surface area ( $\text{m}^2 \text{g}^{-1}$ )	Pore size ( $\text{\AA}$ )	Pore volume ( $\text{cm}^3 \text{g}^{-1}$ )
NA	66.01	24.1	0.09
AA	141	31.9	0.11

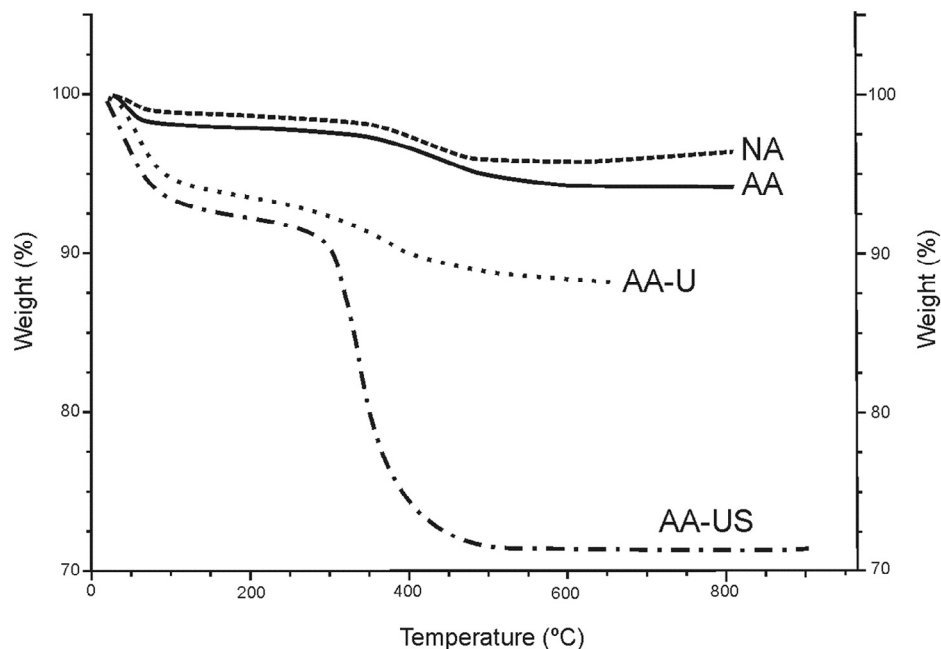


Fig. 4. Thermogravimetric analysis (TGA) traces of raw natural aluminosilicate (NA), activated aluminosilicate (AA), uric acid modified aluminosilicate (AA-U) and uric acid modified aluminosilicate after sulfate absorption (AA-US). Heating rate is  $10\text{ }^{\circ}\text{C min}^{-1}$  in  $\text{N}_2$  atmosphere.

Fig. 5 shows the results of the studies of the adsorption of uric acid onto activated aluminosilicate (AA). The adsorption was essentially completed after the first 4 minutes (70% at minute 2), finally reaching the equilibrium within 60 min

Table 3

Z potential (zP) values of activated aluminosilicate (AA), uric acid modified aluminosilicate (AA-U) and sulfates adsorbed in aluminosilicate-modified uric acid (AA-US).

Sample	Zp (mV)
AA	-36.9
AA-U	-13.5
AA-US	-18

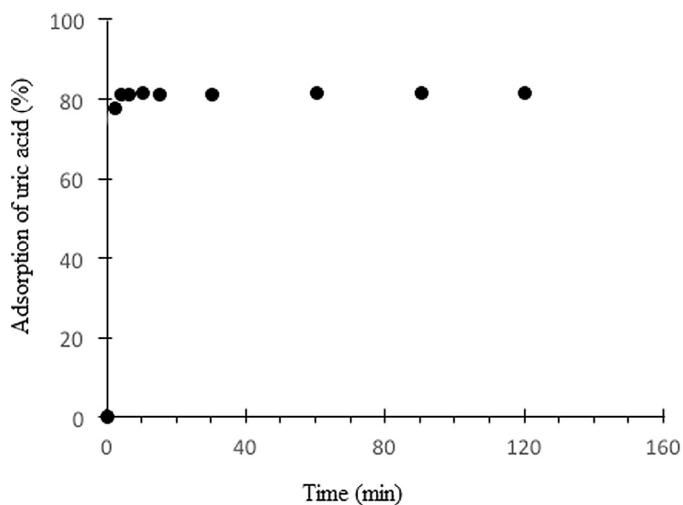


Fig. 5. Effect of contact time on the adsorption of uric acid (113 mg/l concentration) on AA.

followed by a plateau. More than 80% of uric acid (initial concentration 113 mg/l) was successfully up taken by the NA before reaching the equilibrium.

The effect of pH on the adsorption of uric acid on AA is shown in Fig. 6. Increasing the mass of activated aluminosilicate causes an increase in the absorption of sulfates, as expected in all cases. However decreasing the pH the absorption of sulfates is greatly favored. As mentioned before uric acid has two pKa, low pH keeps the uric acid in its acid form while higher pH promotes its ionization [32,33]. Obviously ureate ions have less affinity for the negative charge in aluminosilicate surface so absorption of negatively charged sulfate ions is in fact more efficient at low pH. At this point it is important to mention that pH of normal wastewater is between 6 and 8, so in order to keep conditions that are more likely to occur in a real effluent, next experiments were carried out at pH 7.

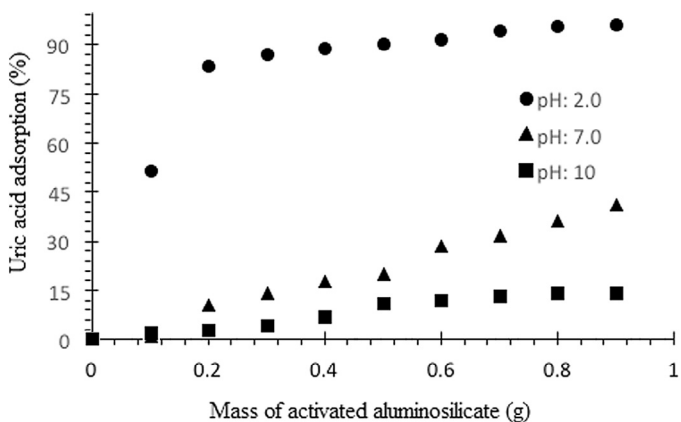


Fig. 6. Effect of pH on the amount of uric acid absorption (initial concentration 400 mg/l) on different amounts of AA.

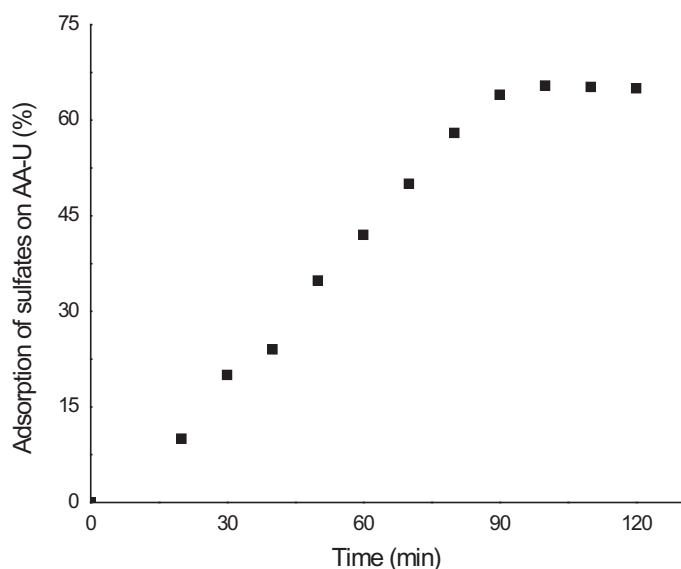


Fig. 7. Effect of contact time on the adsorption of sulfates on AA-U (500 mg/l concentration).

Fig. 7 shows the results of the studies of the adsorption of sulfates on modified aluminosilicate with uric acid (AA-U). The adsorption was essentially completed after 90 minutes (65%), finally reaching the equilibrium within 100 min followed by a plateau. More than 60% of sulfates (initial concentration 500 mg/l) were successfully up taken by the AA-U before reaching the equilibrium.

Isotherm of absorption of sulfates onto AA-U was carried out at pH 7 with an initial concentration of sulfates of 250–500 mg/l (Fig. 8). As it was stated before pH 7 was evaluated because the both lower and higher pH belong to a very specific type of wastewater, being those of pH 7 the most widespread and common.

Data of isotherm absorption of sulfates on AA-US were fit to Langmuir and Freundlich isotherm models to estimate the

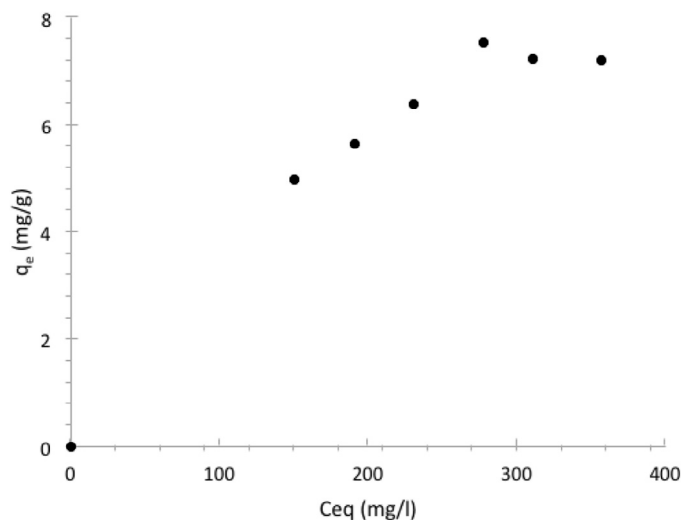


Fig. 8. AA-U adsorption capacity ( $q_e$ ) for sulfates versus sulfate concentration at equilibrium in liquid phase ( $C_{eq}$ ).

Table 4

Constants for the data fitting of sulfate adsorption isotherm on AA-US at pH 7.

	Langmuir				Freundlich			
	$q_{max}$ (mg g <sup>-1</sup> )	b	R <sup>2</sup>	%SD	n	k (mg g <sup>-1</sup> )	R <sup>2</sup>	%SD
AA-US	11	0.7	0.91	0.25	2.9	1.33	0.88	2.39

maximum adsorption capacity of uric acid on AA at pH 7 and 25 °C. Langmuir model is based on the assumption that maximum adsorption corresponds to monolayer formation of adsorbate on the adsorbent surface (sulfates and aluminosilicate, respectively) (Fig. 9). The energy of adsorption is constant and no transmigration of adsorbate occurs on the surface [34]; whereas Freundlich isotherm is used to describe adsorption on both homogeneous and heterogeneous surfaces [35].

Based on the adsorption isotherm the mechanism of sulfate absorption can be divided in two regimes separated by an inflection point when saturation is reached ( $C_{eq}$  around 300 mg/l). Considering the negative charge of AA, protonated uric acid shows affinity for the negative sites of AA at acid pH, as demonstrated before by Z potential measurements. Table 4 shows the values for the constants, deviation standard and linear correlation coefficients for Freundlich and Langmuir isotherm models. Although experimental data seem to fit better to Langmuir model, the correlation is still weak to discriminate between preferential mechanisms of absorption. So in this material at pH 7 it can be concluded that contribution of both Freundlich and Langmuir isotherm models are operating.

#### 4. Conclusions

In this work it was revealed that natural aluminosilicates are able to remove two residues that are commonly found as water contaminates. Uric acid can play the role of efficient modifier of the surface charge, over which the other contaminants, sulfate ions, are absorbed.

In contrast with previous works, in this case widely available natural aluminosilicate is used under conditions that reproduce typical wastewater (pH and concentration of contaminants). Regarding the underlying mechanism of the absorption of sulfates, it is not fully understood, but contribution from both Freundlich and Langmuir is possible. Nevertheless the mechanism can be divided in two regimes separated by an inflection point when saturation is reached.

Although the source of this material is local, its basic structure of aluminosilicate common to other aluminosilicates offers a platform for the use of two contaminants, one playing the role of charge modifier for the subsequent absorption of the other one, e.g. undesirable anions. This work opens the path for a more detailed investigation and optimization of parameters in order to increase the amount of sulfates removed under different conditions. This is a first attempt to demonstrate the use of water contaminants to overcome the use of expensive synthetic adsorbents or/and modifiers for sulfate removal. It is expected that this work impacts the efficient future technologies for wastewater treatment from different industries.

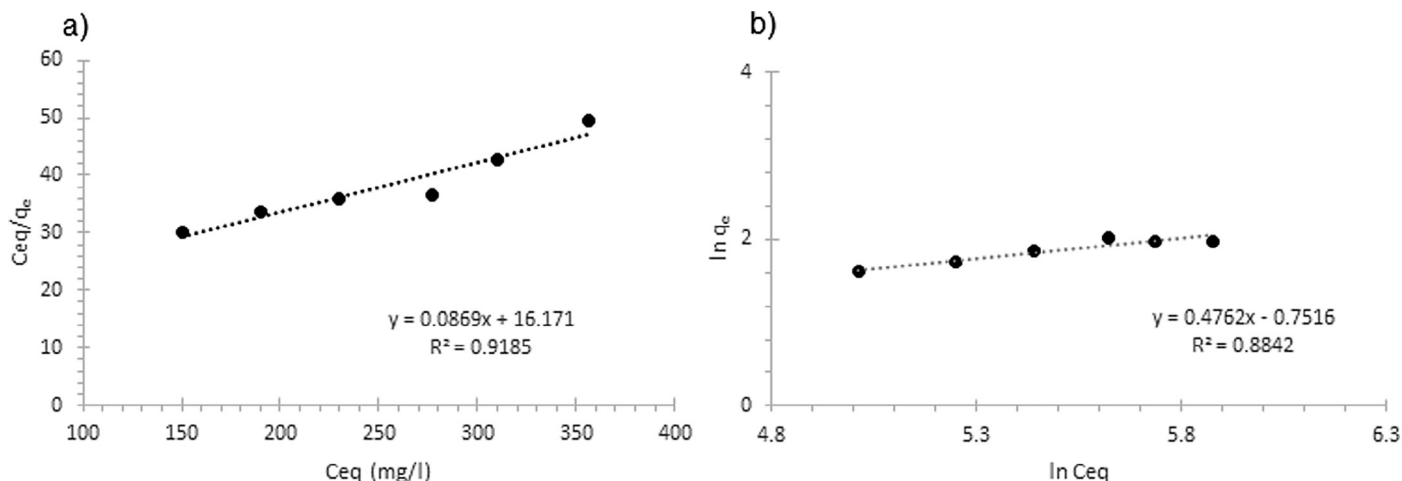


Fig. 9. Comparison between sulfate adsorption experimental data fitting to Langmuir (a) and Freundlich (b) models.

## Acknowledgements

The authors acknowledge funding for this research by CONACYT project 260409 and PAPIIT-UNAM project IT200114 (Mexico); Autonomous University of Baja California; CONACyT scholarship PhD; Government Program «Science» of Tomsk Polytechnic University, grant No. 4.1187.2014/K; and technical support of Israel Gradilla Martinez, Martha Eloisa Aparicio Ceja and Dr. Oxana Martynyuk.

## References

- [1] J.G.V. Rodríguez, A.E. Leal, E. Vélez, L.A. Hurtado, Seasonal Evaluation of the Effluent Quality of the Rosarito, México Wastewater Treatment Plant and Identification of Alternatives for Its Indirect Reuse, Sustainable Development, WITPress Sothampton, United Kingdom, 2009, pp. 571–578.
- [2] WHO, Sulfate in Drinking-water. Background Document for Preparation of WHO Guidelines for Drinking-water Quality, World Health Organization., Geneva, 2003. WHO/SDE/WSH/03.04/114.
- [3] Comisión Nacional del Agua. Estadística del agua en México edición. Secretaría de Medio Ambiente y Recursos Naturales, México D.F., 2011, pp. 8–10.
- [4] CESPT. Comisión Estatal de servicios Públicos de Tijuana (State Public Service Commission of Tijuana). <<http://www.cespt.gob.mx/ServNoticias/ConsultaNoticias.aspx?anio=2014>>, 2014 (accessed 30.11.15).
- [5] L. Heredia Hernández, Master Thesis, “Remoción de N y P por adsorción reactiva con magnesita activada” (Remotion of N and P via reactive adsorption using activated mangesite), UABC, Tijuana B.C. México. 2013.
- [6] M.F. Sierra, Master Thesis, “Remoción de fosfatos con precipitación con calcita en el efluente de una PTAR” (Remotion of phosphates via precipitation using calcite in an PTAR effluent), UABC, Tijuana B.C. México. 2009.
- [7] Z. Amjad, Applications of antiscalants to control calcium sulfate scaling in reverse osmosis systems, Desalination 54 (1985) 263–276.
- [8] M. Panayotova, V. Panayotov, An electrochemical method for decreasing the concentration of sulfate and molybdenum ions in industrial wastewater, J. Environ. Sci Health A Tox Hazard Subst Environ Eng. 39 (2004) 173–183.
- [9] A. Sarti, E. Pozzi, F.A. Chinalia, A. Ono, E. Foresti, Microbial processes and bacterial populations associated to anaerobic treatment of sulfate-rich wastewater, Process Biochem. 45 (2010) 164–170.
- [10] A. Sarti, A.J. Silva, M. Zaiat, E. Foresti, Full-scale anaerobic sequencing batch biofilm reactor for sulfate-rich wastewater treatment, Desalination. Water Treat. 25 (2011) 13–19.
- [11] K. Gedik, I. Imamoglu, Removal of cadmium from aqueous solutions using clinoptilolite: influence of pretreatment and regeneration, J. Hazard. Mater. 155 (2008) 385–392.
- [12] S.S. Gupta, K.G. Bhattacharyya, Immobilization of Pb(II), Cd(II) and Ni(II) ions on kaolinite and montmorillonite surfaces from aqueous medium, J. Environ. Manage. 87 (2008) 46–58.
- [13] S.S. Gupta, K.G. Bhattacharyya, Adsorption of heavy metals on kaolinite and montmorillonite: a review, Phys. Chem. Chem. Phys. 14 (2012) 6698–6723.
- [14] M. Sanchez-Martín, M. Dorado, C. del Hoyo, M. Rodríguez-Cruz, Influence of clay mineral structure and surfactant nature on the adsorption capacity of surfactants by clays, J. Hazard. Mater. 150 (2008) 115–123.
- [15] O. Bouras, J.C. Bollinger, M. Baudu, H. Khalaf, Adsorption of diuron and its degradation products from aqueous solution by surfactant-modified pillared clays, Appl. Clay Sci. 37 (2007) 240–250.
- [16] M.G. da Fonseca, J.S. Barone, C. Airoidi, Clays Clay. Miner. 48 (2000) 638.
- [17] S.L. Burkett, A. Press, S. Mann, Chem. Mater. 9 (1997) 1071.
- [18] K.A. Carrado, L. Xu, R. Csencsits, J.V. Muntean, Chem. Mater. 13 (2001) 3766.
- [19] S.K. Lee, S.J. Kim, Appl. Clay Sci. 22 (2002) 55.
- [20] F. Liu, J. He, C. Colombo, A. Violante, Competitive adsorption of sulfate and oxalate on goethite in the absence or presence of phosphate, Soil Sci. 164 (1999) 180–189.
- [21] L.M. Long, J. Ma, J. Liu, Y.X. Cao, Montmorillonite adsorbs uric acid and increases the excretion of uric acid from the intestinal tract in mice, J. Pharm. Pharmacol. 61 (11) (2009) 1499–1504.
- [22] G.B. Cleveland. Geology of the Otay Bentonite deposit, San Diego County, California. California Division of Mines special report. 1960, p. 64. 16p.
- [23] A.M. Morales-Carrera, Estado del arte de la arcilla de la provincia de Guayas y su proyección a la península de Santa Elena, Ecuador. Bol. Geol. Minero 117 (4) (2006) 723–736.
- [24] E.G. Tuesta, M. Vivas Sun, A. Gutarra, Modificación química de arcillas y su aplicación en la retención de colorantes, Rev. Soc. Quím. Perú 71 (1) (2005) 26–36.
- [25] P.W. Schindler, M. Stadler, The effect of dissolved ligands on the sorption of Cu(II) by Ca-montmorillonite, Clays Clay. Miner. 42 (1994) 148–160.
- [26] D.M. Moore, R.C. Reynolds, X-ray Diffraction and the Identification and Analysis of Clay Minerals, vol. 378, Oxford University Press, Oxford, 1989.

- [27] A. Viani, G. Gualtieri, M. Artioli, The nature of disorder in montmorillonite by simulation of X-ray powder patterns, *Am. Mineral.* 87 (2002) 966–975.
- [28] D. Gournis, A. Lappas, M.A. Karakassides, D. Tobbens, A. Moukarika, A neutron diffraction study of alkali cation migration in montmorillonites, *Phys. Chem. Miner.* 35 (2008) 49–58.
- [29] D. Ikuta, N. Kawame, S. Banno, T. Hirajima, K. Ito, J.F. Rakovan, et al., First in situ X-ray diffraction identification of coesite and retrograde quartz on a glass thin section of an ultrahigh-pressure metamorphic rock and their crystal structure details, *Am. Mineral.* 92 (2007) 57–63.
- [30] R.A. Garay Díaz, M.E. Mena Gómez, Clasificación de Arcillas presentes en los bancos de Guatajiagua, Departamento de Morazán, y Facultad Multidisciplinaria Oriental (Doctoral dissertation, Universidad de El Salvador) 2007, p. 69.
- [31] C. Volzone, R.M. Torres Sanchez, Thermal and mechanical effects on natural and activated smectite structure, *Colloids Surf. A.* 81 (1993) 1–3, 211–216.
- [32] G.D. Fasman, Physical and chemical data, in *CRC Handbook of Biochemistry and Molecular Biology*, third ed., vol. I, CRC Press, Cleveland, 1976, p. 331.
- [33] J.H. Dean, *Lunge's Handbook of Chemistry*, McGraw-Hill, New York, 1985, pp. 5-46–5-60.
- [34] I. Ali, M. Asim, T.A. Khan, Low cost adsorbents for removal of organic pollutants from wastewater, *J. Environ. Manage.* 113 (2012) 170–183.
- [35] H.Z. Freundlich, Über die adsorption in losungen, *Z. Phys. Chem.* 57 (1906) 385–470.